Agonist-promoted heteromeric oligomerization between adenosine A_1 and $P2Y_1$ receptors in living cells

Kazuaki Yoshioka[a,b,1], Osamu Saitoh[a], Hiroyasu Nakata[a,*]

[a] *Department of Molecular Cell Signaling, Tokyo Metropolitan Institute for Neuroscience, 2-6 Musashidai, Fuchu, Tokyo 183-8526, Japan*
[b] *Japan Science and Technology Corporation, Kawaguchi, Saitama 332-0012, Japan*

Received 23 May 2002; accepted 29 May 2002

First published online 20 June 2002

Edited by Julio Celis

Abstract **We have explored the process of oligomerization of G protein-coupled purinergic receptors, adenosine A_1 receptor (A_1R) and $P2Y_1$ receptor ($P2Y_1R$), in intact HEK293T cells by means of modified bioluminescence resonance energy transfer technology ($BRET^2$) that offers greatly improved separation of the emission spectra of the donor and acceptor moieties compared to traditional BRET. This approach identified both constitutive and agonist-promoted heteromeric oligomerization between Myc-tagged $P2Y_1R$ fused to a donor, *Renilla* luciferase (Myc-$P2Y_1R$-Rluc) and HA-tagged A_1R fused to an acceptor, a different form of green fluorescent protein (HA-A_1R-GFP^2). The $BRET^2$ signal increased in a time-dependent manner in the cells expressing HA-A_1R-GFP^2/Myc-$P2Y_1R$-Rluc upon addition of agonists for both receptors, which could be inhibited by pretreatment with the $P2Y_1R$ antagonist MRS2179. A high degree of HA-A_1R-GFP^2 and Myc-$P2Y_1R$-Rluc co-localization in the co-transfected HEK293T cells was also observed by confocal laser microscopy. These results indicate that A_1R and $P2Y_1R$ can form constitutive hetero-oligomers in living cells and this process is promoted by the simultaneous activation of both receptors.**

Key words: Purinergic receptor; Adenosine A_1 receptor; $P2Y_1$ receptor; Hetero-oligomerization; Bioluminescence resonance energy transfer; HEK293T cell

1. Introduction

Purines such as adenosine or ATP are involved in modulating many physiological processes, including cardioprotection, pain, sleep, neurotransmission, and neuromodulation [1]. They exert such diverse biological processes *via* specific cell surface receptors termed purinergic receptors which are divided into two main subfamilies, namely adenosine or P1 receptors and ATP or P2 receptors. The P1 receptors have been further subdivided into A_1, A_{2A}, A_{2B} and A_3, all of which are G protein-coupled receptors (GPCRs). The P2 receptors are also subclassified into $P2X_{(1-7)}$ receptors, which are ligand-gated ion channels, and $P2Y_{(1,2,4,6,11,12)}$ receptors, which are GPCRs. However, despite extensive studies, details of the physiological functions of the purinergic receptor subtypes remain unclear, especially on complex cross-talk interactions in vivo as described in the rat hippocampal neuron [2] and also in the rat portal vein [3].

Recently, a significant number of GPCRs have been shown to exist in homomeric or heteromeric oligomers [4]. It has been suggested that this oligomerization represents a general phenomenon among GPCRs, resulting in a greater diversity of GPCR signaling. In fact, we recently reported that $G_{i/o}$ protein-coupled adenosine A_1 receptors (A_1Rs) and $G_{q/11}$ protein-coupled P2Y receptor, subtype $P2Y_1Rs$ form a heteromeric complex in HEK293T cells where A_1R exerts $P2Y_1R$-like agonistic effects [5]. We therefore speculated that this heteromeric assembly between purinergic receptors produces a hybrid pharmacology that explains the hitherto undefined physiological functions of purines and an increased diversity of purine signaling in various tissues and cells.

In the present study, we took advantage of a recently developed approach, known as BRET (bioluminescence resonance energy transfer) [6], to investigate whether A_1R and $P2Y_1R$ could exist as heteromers in living cells. BRET is strictly dependent on the molecular proximity between the energy donor, *Renilla* luciferase (Rluc), and acceptor, green fluorescent protein (GFP), making it ideal for studying protein–protein interactions. The improved BRET technique ($BRET^2$) that offers greatly improved separation of the emission spectra of the donor and acceptor moieties compared to traditional BRET was employed in this study [7].

2. Materials and methods

2.1. cDNA constructs, cell culture and transfection

The cDNA construct of hemagglutinin (HA)-A_1R-modified green fluorescent protein (GFP^2) and Myc-tagged $P2Y_1R$ (Myc-$P2Y_1R$)-Rluc were generated by amplification of the HA-tagged rat A_1R and Myc-tagged rat $P2Y_1R$ coding sequence [5] without its stop codon using sense and antisense primers containing distinct restriction enzyme sites at the 5′ and 3′ ends, respectively. The fragments were

*Corresponding author. Fax: (81)-42-321 8678.
E-mail address: nakata@tmin.ac.jp (H. Nakata).

[1] Present address: Department of Molecular Vascular Physiology, Kanazawa University Graduate School of Medical Science, 13-1 Takaramachi, Kanazawa, Ishikawa 920-8640, Japan.

Abbreviations: GPCR, G protein-coupled receptor; BRET, bioluminescence resonance energy transfer; FRET, fluorescence resonance energy transfer; $BRET^2$, improved BRET system offered by Perkin-Elmer Life Sciences; GFP^2, modified green fluorescent protein; Rluc, *Renilla* luciferase; A_1R, adenosine A_1 receptor; $P2Y_1R$, $P2Y_1$ receptor; HA, hemagglutinin; HA-A_1R, HA-tagged A_1R; Myc-$P2Y_1R$, Myc-tagged $P2Y_1R$; HA-A_1R-GFP^2, HA-A_1R fused to GFP^2; HA-A_1R-Rluc, HA-A_1R fused to Rluc; Myc-$P2Y_1R$-Rluc, Myc-$P2Y_1R$ fused to Rluc; CPA, N^6-cyclopentyladenosine; ADPβS, adenosine 5′-*O*-(2-thiotriphosphate); MRS2179, N^6-methyl-2′-deoxyadenosine-3′,5′-bisphosphate

0014-5793/02/$22.00
PII: S0014-5793(02)02965-4

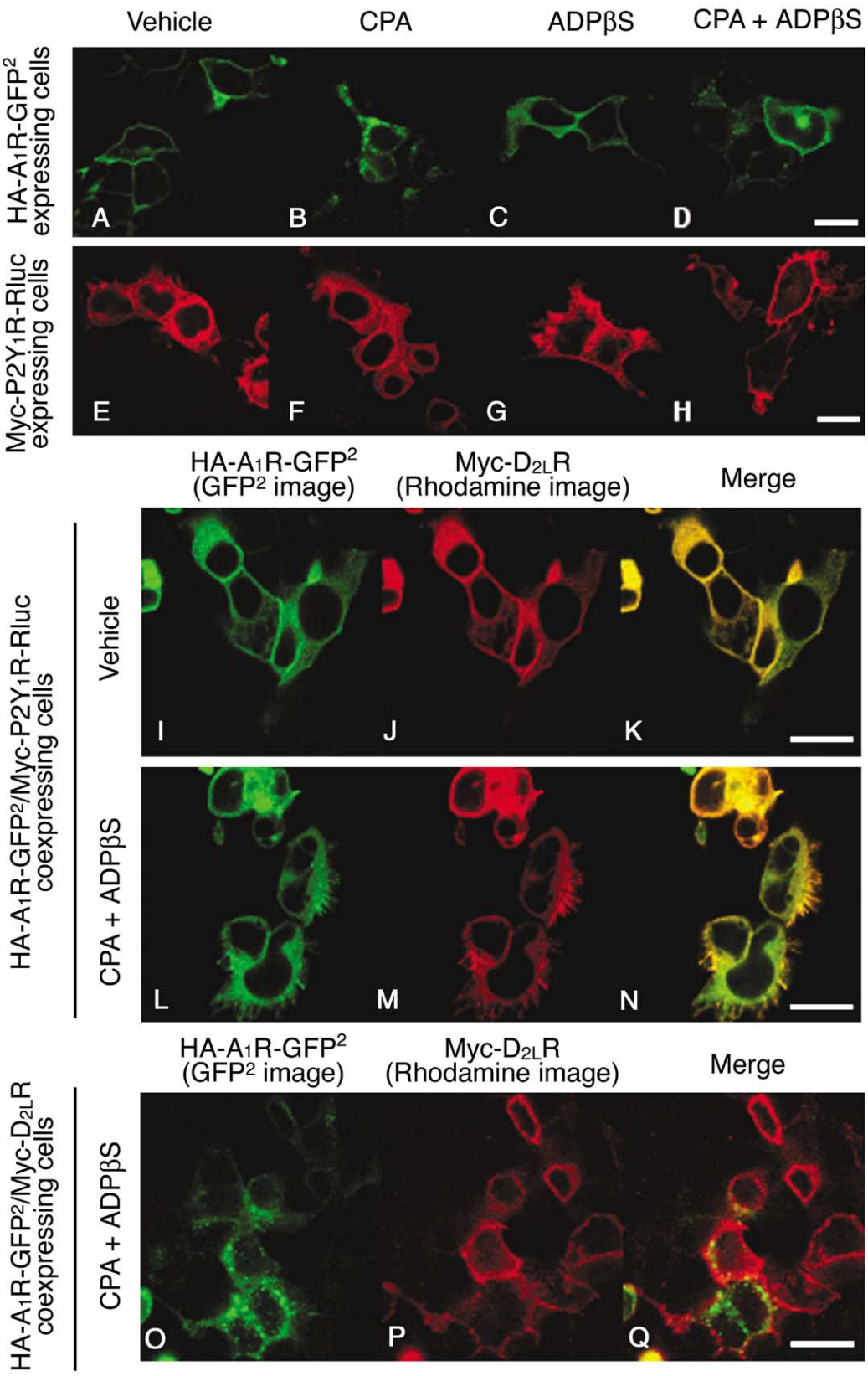

Fig. 1. Double-fluorescence imaging of HA-A_1R-GFP^2 and Myc-$P2Y_1$-Rluc in HEK293T cells. HEK293T cells transfected with HA-A_1R-GFP^2 (A–D) or Myc-$P2Y_1$R-Rluc (E–H) were treated with 1 μM CPA (B,F), 100 μM ADPβS (C,G) or 1 μM CPA+100 μM ADPβS (D,H) for 10 min. Confocal laser microscopy was employed to visualize GFP^2 (green images) and rhodamine (red images). Scale bar, 10 μm. I–Q: Co-localization of HA-A_1R-GFP^2 and Myc-$P2Y_1$-Rluc in HEK293T cells. HA-A_1R-GFP^2/Myc-$P2Y_1$R-Rluc co-transfected HEK293T cells were incubated for 10 min with (L–N) or without (I–K) the agonists (1 μM CPA+100 μM ADPβS). HA-A_1R-GFP^2/Myc-D_{2L}R co-expressing cells were incubated for 10 min with the agonists (1 μM CPA+100 μM ADPβS, O–Q). They were visualized by double-fluorescence imaging with a confocal laser microscope to detect GFP^2 (I,L,O, green images) and rhodamine (J,M,P, red images). GFP^2 and rhodamine images were merged using confocal assistant software to reveal HA-A_1R-GFP^2/Myc-$P2Y_1$R-Rluc co-localization (K,N,Q, yellow images). Scale bar, 10 μm.

then subcloned in-frame into the appropriate sites of the codon humanized pGFP^2-N3 and pRluc-N3 expression vectors (BRET^2, Packard Biosciences), respectively. Rluc and GFP^2 were located at the C-terminal end of the receptors.

HEK293T cells were maintained and were transfected transiently as described previously [5]. Cells were harvested 48 h after transfection and washed twice in ice-cold phosphate-buffered saline (PBS) before co-immunoprecipitation and BRET experiments.

2.2. Confocal laser microscopy and co-immunoprecipitation

Confocal microscopic observations were made with a Zeiss LSM410 confocal microscope. Co-transfected cells were labeled with rhodamine-conjugated anti-Myc monoclonal antibody (1:200, Santa Cruz). GFP^2 and rhodamine were excited using a 488 nm and 543 nm argon/krypton laser and detected with a 510–525 nm bandpass filter and a 560 nm longpass filter, respectively. The images were manipulated with Zeiss LSM software. Co-immunoprecipitation studies were performed as described previously [5].

2.3. BRET^2 assay

Approximately 5×10^5 cells per well suspended in the assay buffer (Dulbecco's PBS containing 0.1 g/l $CaCl_2$, 0.1 g/l $MgCl_2$ and 1 g/l D-glucose) were distributed in a 96-well white-walled microplate (Packard Biosciences). The cells were incubated with or without receptor ligands for specific periods at 37°C. The coelenterazine derivative DeepBlue C (Packard Biosciences), Rluc substrate, was added at a final concentration of 5 μM and signal was detected immediately by using a fusion microplate analyzer (Packard Biosciences) with 410 and 515 nm emission filters. Background was taken as the area of this region of the spectrum without transfectants. Data are represented as a BRET ratio defined as [(emission at 515 nm)−(background emission at 515 nm)]/[(emission at 410 nm)−(background emission at 410 nm)].

3. Results

3.1. Co-localization of A_1R and $P2Y_1R$ and their agonist-induced translocation in HEK293T cells

Localization of HA-tagged A_1R (HA-A_1R)-GFP^2 in the plasma membrane of HEK293T cells expressing HA-A_1R fused to GFP^2 (HA-A_1R-GFP^2) alone is shown in Fig. 1A–D. Addition of N^6-cyclopentyladenosine (CPA) to the transfected cells resulted in the appearance of intense punctate areas of signal on the plasma membrane, suggesting a clustering of HA-A_1R-GFP^2 (Fig. 1B,D). Vehicle or CPA addition showed a broad distribution of Myc-$P2Y_1R$ on the surface of Myc-$P2Y_1R$ fused to Rluc (Myc-$P2Y_1R$-Rluc)-transfected HEK293T cells (Fig. 1E,F), whereas either adenosine 5′-*O*-(2-thiotriphosphate) (ADPβS)- or combined-agonist-treated cells revealed a structure where $P2Y_1R$ accumulated to plasma membranes and a microspike-like structure was present on the surface of cells (Fig. 1G,H).

A homogeneous co-localization of HA-A_1R-GFP^2 and Myc-$P2Y_1R$-Rluc on the plasma membrane was observed in vehicle-treated (Fig. 1I–K) and also in CPA-treated cells (data not shown). When cells were treated with CPA+ADPβS, a redistribution and co-localization of these receptors were observed (Fig. 1L–N). Clusters of HA-A_1R-GFP^2, seen as the punctate accumulation of GFP^2 signals as shown in Fig. 1B,D, disappeared and were translocated to the plasma membrane (Fig. 1L). Microspikes were present on the cell surface where co-localization between HA-A_1R-GFP^2 and Myc-$P2Y_1R$-Rluc was shown to be very intense (Fig. 1N, yellow). These agonist-dependent translocation shown in Fig. 1L–N was not observed in HA-A_1R/Myc-$D_{2L}R$-Rluc coexpressing cells (Fig. 1O–Q), indicating that A_1R and $P2Y_1R$ co-operate together via the same trafficking pathway.

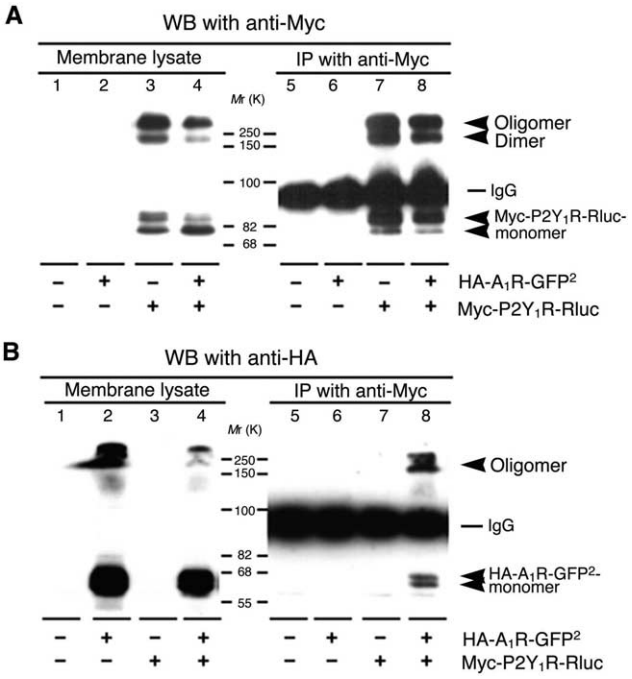

Fig. 2. Co-immunoprecipitation of HA-A_1R-GFP^2 and Myc-$P2Y_1R$-Rluc expressed in HEK293T cells. Cell lysates were immunoprecipitated with anti-Myc antibodies, and samples resolved by SDS–PAGE and immunoblotted with anti-Myc (A, right panel) or anti-HA (B, right panel) antibodies. Cell lysates (left panels of A, B) were prepared from HKE293T cells transiently expressing the indicated receptors. Myc-$P2Y_1R$-Rluc (upper column, lanes 3, 4) and HA-A_1R-GFP^2 (lower column, lanes 2, 4) were detected by anti-Myc and anti-HA antibodies, respectively. In addition to Myc-$P2Y_1R$-Rluc (A, lanes 7, 8), anti-Myc antibodies immunoprecipitated HA-A_1R-GFP^2 from cell membrane lysates co-expressing HA-A_1R-GFP^2/Myc-$P2Y_1R$-Rluc (B, lane 8). Data are representative of four independent experiments.

3.2. Association of HA-A_1R-GFP^2 and Myc-$P2Y_1R$-Rluc in HEK293T cells assessed by co-immunoprecipitation

Western blots of cell membrane lysates expressing Myc-$P2Y_1R$-Rluc exhibited anti-Myc reactive bands of 76 and 84 kDa near the predicted molecular mass in addition to bands of 160 and >250 kDa (Fig. 2A, lanes 3,4). Western blots of cell membrane lysates expressing HA-A_1R-GFP^2 showed anti-HA antibody reactive bands of 59 and 66 kDa in addition to bands of a potential dimer and oligomer (Fig. 2B, lanes 2,4). We found that anti-Myc antibody co-immunoprecipitated HA-A_1R-GFP^2 (Fig. 2B, lane 8) in addition to Myc-$P2Y_1R$-Rluc (Fig. 2A, lane 8) from cells co-expressing HA-A_1R-GFP^2/Myc-$P2Y_1R$-Rluc. Conversely, anti-HA antibody immunoprecipitated HA-A_1R-GFP^2 with Myc-$P2Y_1R$-Rluc (data not shown). These results indicate that constitutive hetero-oligomerization between A_1R and $P2Y_1R$ can occur not only with HA-A_1R and Myc-$P2Y_1R$ tagged with short peptides [5] but also between HA-A_1R-GFP^2 and Myc-$P2Y_1R$-Rluc when expressed as fusion proteins.

3.3. Association of HA-A_1R-GFP^2 and Myc-$P2Y_1R$-Rluc in HEK293T cells assessed by BRET^2

To determine whether there is a constitutive association between A_1R/A_1R or A_1R/$P2Y_1R$ in living cells, BRET^2 was measured in HEK293T cells co-transfected with either HA-A_1R-GFP^2/HA-A_1R fused to Rluc (HA-A_1R-Rluc) or

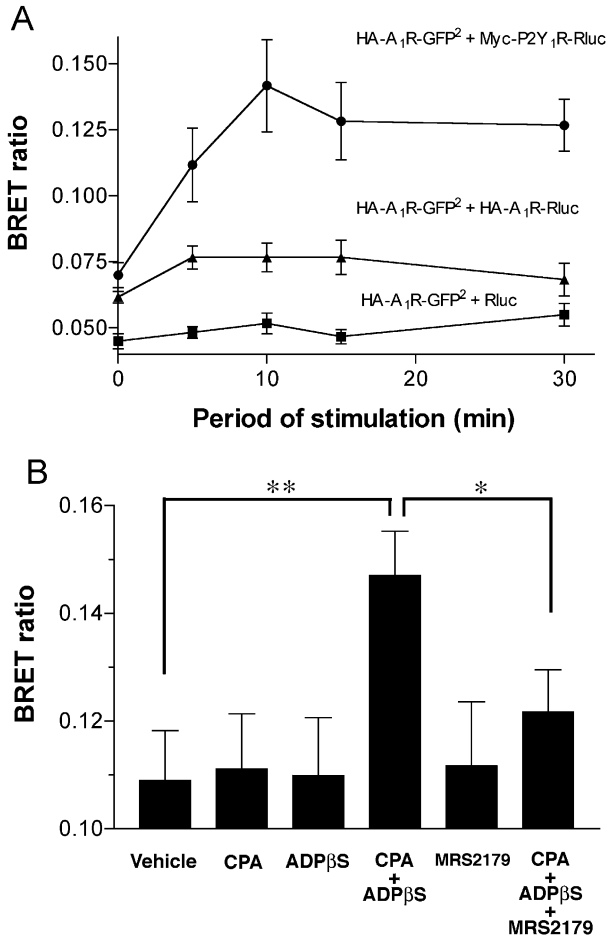

Fig. 3. BRET^2 detection of HA-A_1R-GFP^2 and Myc-P2Y_1R-Rluc in living cells. A: Time-dependent BRET signal in living HEK293T cells co-expressing HA-A_1R-GFP^2 and HA-A_1R-Rluc (homo-oligomer, triangle), HA-A_1R-GFP^2 and Myc-P2Y_1R-Rluc (hetero-oligomer, circle) or HA-A_1R-GFP^2 and Rluc (control, square). Cells were incubated with agonists of A_1R and P2Y_1R (1 μM CPA+100 μM ADPβS) before the addition of Rluc substrates. The data shown represent the mean ± S.E.M. of three independent experiments performed in triplicate for each time point. B: BRET ratio was measured in HEK293T cells co-transfected with HA-A_1R-GFP^2 and Myc-P2Y_1R-Rluc. Cells were incubated with either CPA (1 μM), ADPβS (100 μM), P2Y_1R antagonist MRS2179 (1 mM) or a combination thereof for 10 min before the addition of Rluc substrate. The data represent the mean ± S.E.M. of three independent experiments, $^{**}P < 0.01$ compared with vehicle treatment (control), $^{*}P < 0.05$ compared with CPA and ADPβS treatment (GraphPad Prism 3).

HA-A_1R-GFP^2/Myc-P2Y_1R-Rluc. As shown in Fig. 3A, co-expression of HA-A_1R-GFP^2/HA-A_1R-Rluc (BRET ratio = 0.062 ± 0.004, $n = 15$) or HA-A_1R-GFP^2/Myc-P2Y_1R-Rluc (BRET ratio = 0.07 ± 0.008, $n = 20$) upon addition of Rluc substrates resulted in a small but significant increase in the BRET ratio ($P < 0.05$ versus control cells) under basal conditions. Co-expression of the isolated Rluc along with HA-A_1R-GFP^2 resulted in a weak energy transfer (BRET ratio = 0.045 ± 0.005, $n = 6$), indicating that there was no direct interaction between these two constructs (Fig. 3A, lower line). Similarly, co-expression of isolated GFP^2 with Myc-P2Y_1R-Rluc failed to produce a significant energy transfer signal (BRET ratio = 0.048 ± 0.006, $n = 6$; data not shown). These results provide strong evidence of an actual association between either A_1R-GFP^2 and A_1R-Rluc or A_1R-GFP^2 and P2Y_1R-Rluc in intact cells. The extent of the heteromeric association is substantially greater than that of the homomeric association of A_1R ($P < 0.05$). Incubation of HA-A_1R-GFP^2/Myc-P2Y_1R-Rluc-co-transfected cells with the agonists CPA and ADPβS increased the BRET ratio with a maximum being reached at 10 min (Fig. 3A, upper line). The agonist-promoted BRET signal observed between HA-A_1R-GFP^2 and Myc-P2Y_1R-Rluc did not result from non-specific association between the GFP^2 and Rluc proteins since no increase in the signal intensity was detected in cells expressing either HA-A_1R-GFP^2/Rluc or HA-A_1R-GFP^2/HA-A_1R-Rluc as shown above. It was also confirmed that the BRET signal did not strengthen in cells co-expressing GFP^2 and Rluc (0.045 ± 0.008, $n = 6$). Incubation of HA-A_1R-GFP^2/HA-A_1R-Rluc expressing cells with agonists did not result in a significant increase in the BRET signal (Fig. 3A, middle line).

To demonstrate the specificity of the agonist-dependent increase in the BRET ratio, HA-A_1R-GFP^2/Myc-P2Y_1R-Rluc-transfected cells were incubated for 10 min in the presence of several ligands (Fig. 3B). A significant increase in the ratio was again observed in the presence of both agonists, but not with either alone. This increase was significantly inhibited by pretreatment with N^6-methyl-2′-deoxyadenosine-3′,5′-bisphosphate (MRS2179), a potent P2Y_1R antagonist, although the addition of MRS2179 alone had no effect on the BRET ratio. We then examined whether the increase in heteromeric formation between HA-A_1R-GFP^2 and Myc-P2Y_1R-Rluc induced by the agonists was also detectable in immunoprecipitation experiments. No significant increase in the amount of bound counter receptor proteins was observed (data not shown). It is possible that the agonist-dependent oligomerization might be weak association which could not be detected by the co-immunoprecipitation technique employed in this study, although it remains to be further examined to address this speculation.

4. Discussion

There has been an increasing number of reports describing the existence and functional importance of homo- and hetero-oligomerization of GPCRs (see review [4]). However, the mechanism of the oligomerization is still largely unknown, and it is not clear whether such oligomers persist at the cell membranes and whether the binding of agonist ligands regulates oligomerization. To answer these questions, co-immunoprecipitation strategies seem limited because the solubilization of hydrophobic proteins such as GPCRs can cause artifactual aggregations or the solubilization process itself can inhibit the association between GPCRs.

In this study, we first performed a confocal microscopy to observe the co-localization of A_1R and P2Y_1R in HEK293T cells and then utilized a biophysical method, BRET^2, to demonstrate that A_1R and P2Y_1R can undergo agonist-dependent hetero-oligomerization in living cells.

The cluster formation of HA-A_1R-GFP^2 by A_1R agonist, CPA, was attenuated by co-transfection with Myc-P2Y_1R-Rluc (Fig. 1L), suggesting a mechanism by which P2Y_1R negatively regulates the ligand-induced clustering of A_1R. Saura et al. [8] recently reported that the cluster formation of A_1R was accelerated by the presence of either an A_1R agonist or by adenosine deaminase treatment. The distribu-

tion of Myc-$P2Y_1R$-Rluc was significantly altered by the addition of the $P2Y_1R$ agonist, ADPβS. The translocated Myc-$P2Y_1R$-Rluc appeared in both plasma membranes and microspike-like structures on the cell surface (Fig. 1G,H). Although co-localization of HA-A_1R-GFP^2 with Myc-$P2Y_1R$-Rluc was demonstrated regardless of the receptor activation (Fig. 1K,N), it was clearly demonstrated that these receptors co-localized in the microspike-like structures in the presence of ADPβS (Fig. 1N). It should also be noted that $P2Y_1R$ is involved in ADP-induced platelet shape change [9].

Direct interaction between HA-A_1R-GFP^2 and Myc-$P2Y_1R$-Rluc in intact cells was observed by a $BRET^2$ technique that offers greatly improved separation of the emission spectra of the donor and acceptor moieties compared to traditional BRET [7,10]. It should be noted that even small BRET ratio can be determined quantitatively with this system due to its low background. As shown in Fig. 3, receptor stimulation led to a time-dependent increase in the amount of energy transfer in cells co-expressing HA-A_1R-GFP^2/Myc-$P2Y_1R$-Rluc in addition to energy transfer in a constitutive association between these receptors. Interestingly, such a ligand-dependent promotion of $BRET^2$ signaling requires agonists for both receptors (Fig. 3B). The effect of the agonists on the BRET ratio is consistent with the notion that agonists promote the formation of hetero-oligomers [11]. Because ADPβS is a hydrophilic ligand that cannot permeate the plasma membrane, the results indicate that the heteromeric assembly of receptors occurs at the cell surface, influenced by specific receptor activation. A significant inhibition with the $P2Y_1R$ selective antagonist MRS2179 suggests that receptor activation is indeed involved in this agonist-promoted oligomerization (Fig. 3B). Our results also revealed that the A_1R homo-oligomer is present in living HEK293T cells co-expressing A_1R-GFP^2 and A_1R-Rluc, although this homodimer formation seems to be agonist-independent. The presence of homodimer between A_1R has also been suggested by Western blot experiments (Fig. 2B and [12]). Human β_2-adrenergic receptors are similarly reported to form constitutive and agonist-dependent homodimers when expressed in HEK293 cells as determined by traditional BRET [13]. In contrast, using a similar BRET technique, it was found that the human δ-opioid receptor forms homo-oligomers constitutively that were not further regulated by ligand occupancy [11].

It has been shown in immunoprecipitation experiments that A_1R/dopamine D_1 receptor hetero-oligomerization in co-transfected fibroblast cells disappeared on pretreatment with D_1 receptor agonist but not combined pretreatment with D_1 receptor and A_1R agonists [14]. McVey et al. [11] have reported that the hetero-oligomer of δ-opioid receptor and β_2-adrenoreceptor accumulated in the presence of an agonist for either receptor. These observations suggest that the role of agonist occupancy of receptors in homo- or hetero-oligomerization of GPCRs can differ between receptors. The present result in the $BRET^2$ experiment that combined agonists further promoted hetero-oligomerization of two purinergic receptors may support this observation. It remains to be determined whether such agonist-dependent changes in the heteromeric association of A_1R and $P2Y_1R$ constitute important physiological roles in the nervous system where both receptors are highly expressed. The diversity of purinergic functions may indicate a greater number of purinergic receptor subtypes than has been revealed in cloning studies [15–19]. The heteromerization described here may be one of the mechanisms that control such purinergic functions.

Acknowledgements: We are grateful to Dr. K. Nishi for help with confocal microscopy. This work was supported in part by grants for Scientific Research from the Ministry of Education, Science, Sports and Culture of Japan (to O.S. and H.N.), by the Kato Memorial Bioscience Foundation (to O.S.) and also by a Research Grant from the Yamanouchi Foundation for Research on Metabolic Disorders (to H.N.).

References

[1] Ralevic, V. and Burnstock, G. (1998) Pharmacol. Rev. 50, 413–492.
[2] Ikeuchi, Y., Nishizaki, T., Mori, M. and Okada, Y. (1996) Eur. J. Pharmacol. 304, 191–199.
[3] Guibert, C., Loirand, G., Vigne, P., Savineau, J.-P. and Pacaud, P. (1998) Br. J. Pharmacol. 123, 1732–1740.
[4] Bouvier, M. (2001) Nat. Rev. Neurosci. 2, 274–286.
[5] Yoshioka, K., Saitoh, O. and Nakata, H. (2001) Proc. Natl. Acad. Sci. USA 98, 7617–7622.
[6] Xu, Y., Piston, D.W. and Johnson, C.H. (1999) Proc. Natl. Acad. Sci. USA 96, 151–156.
[7] Parent, S., Normand, C., Joly, E., Ménard, L. and Houle, B. Application Note # BRT-001: Bioluminescence Resonance Energy Transfer ($BRET^2$). Principles, Applications, and Products. Packard Bioscience.
[8] Saura, C.A., Mallol, J., Canela, E.I., Lluis, C. and Franco, R. (1998) J. Biol. Chem. 273, 17610–17617.
[9] Jin, J., Daniel, J.L. and Kunapuli, S.P. (1998) J. Biol. Chem. 273, 2030–2034.
[10] Ramsay, D., Kellett, E., McVey, M., Rees, S. and Milligan, G. (2002) Biochem. J. (in press), DOI: 10.1042/BJ20020251.
[11] McVey, M., Ramsay, D., Kellett, E., Rees, S., Wilson, S., Pope, A.J. and Milligan, G. (2001) J. Biol. Chem. 276, 14092–14099.
[12] Ciruela, F., Casadó, V., Mallol, J., Canela, E.I., Lluis, C. and Franco, R. (1995) J. Neurosci. Res. 42, 818–828.
[13] Kroeger, K.M., Hanyaloglu, A.C., Seeber, R.M., Miles, L.E.C. and Eidne, K.A. (2001) J. Biol. Chem. 276, 12736–12743.
[14] Ferré, S., Torvinen, M., Antoniou, K., Irenius, E., Civelli, O., Arenas, E., Fredholm, B.B. and Fuxe, K. (1998) J. Biol. Chem. 273, 4718–4724.
[15] Shinozuka, K., Bjur, R.A. and Westfall, D.P. (1988) Naunyn-Schmiedeberg's Arch. Pharmacol. 338, 221–227.
[16] Saitoh, Y. and Nakata, H. (1996) Biochem. Biophys. Res. Commun. 219, 469–474.
[17] Mendoza-Fernandez, V., Andrew, R.D. and Barajas-López, C. (2000) J. Pharmcol. Exp. Ther. 293, 172–179.
[18] Barajas-López, C., Muller, M.J., Prieto-Gómez, B. and Espinosa-Luna, R. (1995) J. Pharmcol. Exp. Ther. 274, 1238–1245.
[19] Koizumi, S. and Inoue, K. (1997) Br. J. Pharmacol. 122, 51–58.